EUROPEAN JOURNAL OF PURE AND APPLIED MATHEMATICS
2025, Vol. 18, Issue 4, Article Number 6596
ISSN 1307-5543 – ejpam.com
Published by New York Business Global

Stability and Optimal Control Analysis of an $SEIQR$ Epidemic Model with Saturated Incidence Rate

Noshi Gul[1], Ismail Shah[2], Saeed Ahmad[1,*], Ihsan Ullah[1], Manuel De la Sen[3]

[1] *Department of Mathematics, University of Malakand, Chakdara, Dir(L), 18800, Pakistan*
[2] *Department of Mathematics, University of Nottingham Ningbo China, 199 Taikang East Road, Ningbo 315100, China*
[3] *Department of Electricity and Electronics, Institute of Research and Development of Process, University of the Basque Country, Campus of Leioa (Bizkaia), Leioa 48940, Spain*

Abstract. In this article, we proposed a new mathematical model to investigate the dynamics of the infectious disease, control, and general disease transmission. The model exhibits two distinct non-trivial equilibrium states. As a fundamental prerequisite for stability analysis, we first derive the epidemiological threshold parameter R_0 through next-generation matrix methodology. According to our investigation, R_0 plays an essential role in describing the model's dynamics. We demonstrate that in the case when R_0 takes values less or greater than unity, the endemic (disease-free) condition is asymptotically stable both locally and globally. To try to stop the general disease from spreading throughout a community, we add control parameters, create a control model, and suggest control techniques. The maximum principle of Pontryagin is used to derive the optimality system. Finally, the numerical simulations are performed using the fourth-order Runge-Kutta technique to validate and confirm our analytical conclusions. Phase portrait analysis further illustrates the convergence of system trajectories toward disease-free or endemic equilibria under different control scenarios, reinforcing the stability criteria derived for R_0.

2020 Mathematics Subject Classifications: 92D30, 93C15, 93D20, 34D23

Key Words and Phrases: Mathematical model, epidemic disease, asymptotical stability, optimal control theory, phase portrait, numerical simulation

1. Introduction

Infectious diseases are one of the main causes of mortality around the globe. Infectious diseases have existed for as long as humans have been on earth. Due to the emergence and reemergence of some catastrophic diseases in recent decades, infectious diseases have attracted the attention of many researchers [1–5] The main challenges regarding infectious

*Corresponding author.
DOI: https://doi.org/10.29020/nybg.ejpam.v18i4.6596

Email addresses: noshiguluom@gmail.com (N. Gul), ismail8leu@gmail.com (I. Shah), saeedahmad@uom.edu.pk (S. Ahmad), ihsansf3@gmail.com (I. Ullah), manuel.delasen@ehu.eus (M. De la Sen)

diseases include studying the nature of their spread by considering possible factors causing the diseases and predicting their future states. One way is to express these relations in mathematical language. To look into it the mechanisms of infectious disease transfer and forecast its future spread, mathematical models are crucial [6]. The estimation of parameters, the development and testing of hypotheses that aid in disease prediction and disease control are some of the fundamental characteristics of mathematical models. The health department can use the mathematical model's valuable guidelines to take action towards the control and eradication of diseases, which is one of its most significant features. Such models are helpful for identifying how people are simultaneously infected with a disease and what strategy should be used to treat the condition brilliantly. Mathematical modelling is one of the effective methods for predicting the dynamics of infectious diseases in the realm of applied sciences. Numerous publications have been read to research the dynamics and control of numerous infectious diseases [7–9] using mathematical modelling of infectious diseases, which has a rich literature [10–15]. In order to research how to control the transmission of viruses, some modified epidemic models are developed due to the strong resemblance between software viruses and viruses that are living. The results of the investigation have shown how crucial the incidence rate is to understanding the nature of epidemic models [16]. Mathematical modeling uses various incident rates to study the transmission dynamics of infectious disease [17]. Let h denote the disease transmission rate, S and I are respectively used for susceptible and infected individuals. The ratio hSI denotes an incidence rate, known as the bilinear incidence rate. This type of incidence rate is used in various epidemic models [18–21]. The saturated incidence rate $\frac{hSI}{1+\alpha I}$ was first proposed by Capasso and Serlo [22]. Whereas $\frac{hI}{1+\alpha I}$ tends to a saturation level when I is big hI measures the force of infection when the disease is entering a fully susceptible population, and $\frac{1}{1+\alpha I}$ measures the inhibition effect from behavioural changes in susceptible individuals as their numbers rise or from the overpopulation effect of the infected people. Due to the inclusion of the behavioral changes and crowding effects of the infected peoples and the prevention of the contact rate's unboundedness by the selection of acceptable parameters, this incidence rate is more rational than the bilinear incidence rate and has been utilized in numerous pandemic simulations.

2. Model Formulation

In this section, we construct a general disease model and partition the total population $N(t)$ into five parts: S specially the susceptible individuals, E the Exposed people, I the infectious density, Q the quarantine density, and R the people which recovered from disease. The saturated incidence rate $\frac{hSI}{1+\alpha I}$ is adopted to enhance biological realism. Unlike the bilinear form hSI, it incorporates saturation effects: as the infected population I grows, the term $\frac{1}{1+\alpha I}$ models reduced transmission due to behavioral changes or limited contact capacity. This prevents unrealistic unbounded growth in infection force, offering a more accurate representation of real-world epidemic dynamics. The suggested general disease

model is represented by the set of autonomous differential equations below:

$$\begin{cases} \dfrac{dS}{dt} = g - \dfrac{hSI}{1+\alpha I} - (m+b_1)\,S, \\ \dfrac{dE}{dt} = \dfrac{hSI}{1+\alpha I} - (m+c+b_2)\,E, \\ \dfrac{dI}{dt} = cE - (m+b_3+q+\mu)\,I, \\ \dfrac{dQ}{dt} = b_1S + b_2E + b_3I - (m+p)Q, \\ \dfrac{dR}{dt} = qI + pQ - mR. \end{cases} \tag{1}$$

The system indicated above is subject to the following preconditions. $S(0) > 0$, $E(0) \geq 0$, $I(0) \geq 0$, $Q(0) \geq 0$, $R(0) \geq 0$.
$N(t) = S + E + I + Q + R$ displays the total size of the community.
With the use of the derivative and model (3.0.1), we can

$$\frac{dN}{dt} = g - mS - mE - mI - mQ - mR - \mu I = g - m(S+E+I+Q+R) - \mu I.$$

However, $S + E + I + Q + R = N$, the final equation has the following form:

$$\frac{dN}{dt} = g - mN - \mu I.$$

This may be stated even more simply as:

$$\frac{dN}{dt} \leq g - mN. \tag{2}$$

The final inequality can be solved as follows by integrating with respect to t and using the provided initial conditions:

$$N(t) = \frac{g}{m} + Ce^{-mt}.$$

Simplifying further and using the initial conditions $N(0) = N_0$, we obtain

$$N(t) \leq \frac{g}{m} + \left[N(0) - \frac{g}{m}\right]e^{-mt}.$$

On re-arranging we have,

$$N(t) \leq \frac{g}{m}(1 - e^{-mt}) + N(0)e^{-mt}$$

It is confirmed by initial conditions that $N(0) \geq 0$. It may also be noted from the last inequality that the feasible area of the system is reached when the total population $N(t)$ remains positive and bounded.

3. Positivity of Solution

This proves that every phase pathway that begins in the positive area R^5 ultimately occurs in the phase space reaches and remains in the possibility area triangle (the model falls into the biologically possible area). This can be accomplished by demonstrating that the triangle is a positively invariant set and the systems global attractor. The positivity of the proof is determined by the following theorem.

Theorem 1. *The system (1) novel general disease model has a positive solution for all beginning values that are supplied.*

Proof. The first equation in the model, may be extracted as follows.

$$\frac{dS}{dt} = g - \frac{hSI}{1+\alpha I} - (m+b_1)\,S.$$

This can be written as:

$$\frac{dS}{dt} \geq (\lambda(t) + (m+b_1))S \geq g,$$

By using the given initial conditions, this first order differential equation's solution is provided as:

$$S(t) \geq e^{-(m+b_1)t - \int_0^t \lambda(t)dt}\left(S(0) + g\int_0^t [e^{(m+b_1)t_1 + \int_0^t \lambda(t)dt}]\right).$$

Due to the fact that under integration all the constants in the suggested model are positive which possesses the nonnegativity in both the invariant and results:

$$\triangle = \left\{S(t), E(t), I(t), Q(t), R(t) \in R^5 \ : \ S \ > `0(E, I, Q, R \geq 0), N(t) \ \leq \ \frac{g}{m}\right\}.$$

4. Steady States

To determine how the suggested model behaves qualitatively, there are two different kinds of stable states: endemic equilibriums and equilibriums absence of illness. The endemic equilibrium point is represented by E^1, while the equilibrium point devoid of illness is represented by E^0.

4.1. Disease Free Equilibrium point, E^0

The disease-free stationary point designates the location at which the illness has been totally eradicated from the local population. For the suggested model's no-disease equilibrium to be found, given that the illness is not found in the population, every equation has a zero on its right hand, resulting in $E = I = 0$. The no-sickness stationary point is achieved by computation and is denoted by E^0, as seen below:

$$E^0 = (S^0, E^0, I^0, Q^0, R^0) = \left(\frac{g}{m+b_1}, 0, 0, \frac{b_1 g}{(m+p)(m+b_1)}, \frac{b_1 gp}{m(m+p)}\right).$$

4.2. Endemic Equilibria

According to the endemic equilibrium, this occurs when the illness affects a community for a lengthy period of time. We shall put the right side of the proposed model equal to zero in order to locate the endemic equilibria. The endemic equilibria for the system (3.0.1) at $E^1 = (S^*, E^*, I^*, Q^*, R^*)$ are

$$\begin{cases} S^* = \dfrac{(m+c+b_2)(m+b_3+q+\mu)(1+\alpha I^*)}{hc}, \\ E^* = \dfrac{(m+b_3+q+\mu)I^*}{c}, \\ I^* = \dfrac{hgc-(m+b_1)(m+b_2+c)(m+b_3+q+\mu)}{(m+b_2+c)(m+b_3+q+\mu)(h+\alpha(m+b_1))}, \\ Q^* = \dfrac{b_1S^*+b_2E^*+b_3I^*}{m+p}, \\ R^* = \dfrac{qI^*+pQ^*}{m}. \end{cases}$$

4.3. Basic Threshold Number

The basic reproduction number R_0 is defined as the average number of secondary infections produced by one infected individual in a completely susceptible population. This time, R_0 is calculated as typically there are how many secondary cases of general illness peeople that an individual with a general disease who was not receiving treatment throughout his or her general disease caused in a population of potential general disease patients.

The well-known next generation matrix may be used to establish the fundamental reproduction number. For this, we separate patients who are infected and those who are not. According to model, the infected classes are E and I. Consider only those classes which infection of the disease posses, the model becomes

$$J_1 = (E, I),$$

$$\frac{dJ_1}{dt} = \frac{d}{dt}(E, I).$$

$$\begin{aligned} \frac{dE}{dt} &= \frac{hSI}{1+\alpha I} - (m+c+b_2)E, \\ \frac{dI}{dt} &= cE - (m+b_3+q+\mu)I. \end{aligned} \tag{3}$$

Using the system's making the matrices $\mathcal{F}$ and $\mathcal{V}$ which show the susceptible people and infected people.

$$\frac{dx}{dt} = \mathcal{F} - \mathcal{V},$$

Where,

$$\mathcal{F} = \begin{bmatrix} \frac{hSI}{1+\alpha I} \\ 0 \end{bmatrix}, \qquad \mathcal{V} = \begin{bmatrix} (m+c+b_2)E \\ -cE + (m+b_3+q+\mu)I \end{bmatrix},$$

Then by finding the maximum spectram of the system $F^*V^{-1^*}$

$$R_0 = \frac{hcg}{(m+b_1)(m+c+b_2)(m+b_3+q+\mu)}.$$

which is the basic reproductive value R_0.

The basic reproduction number R_0 acts as a key epidemiological threshold governing system dynamics. If $R_0 < 1$, the disease-free equilibrium is both locally and globally asymptotically stable, leading to disease eradication. If $R_0 > 1$, the disease-free equilibrium becomes unstable, and the endemic equilibrium is asymptotically stable, reflecting disease persistence. Thus, R_0 directly determines the long-term behavior of the infection within the population.

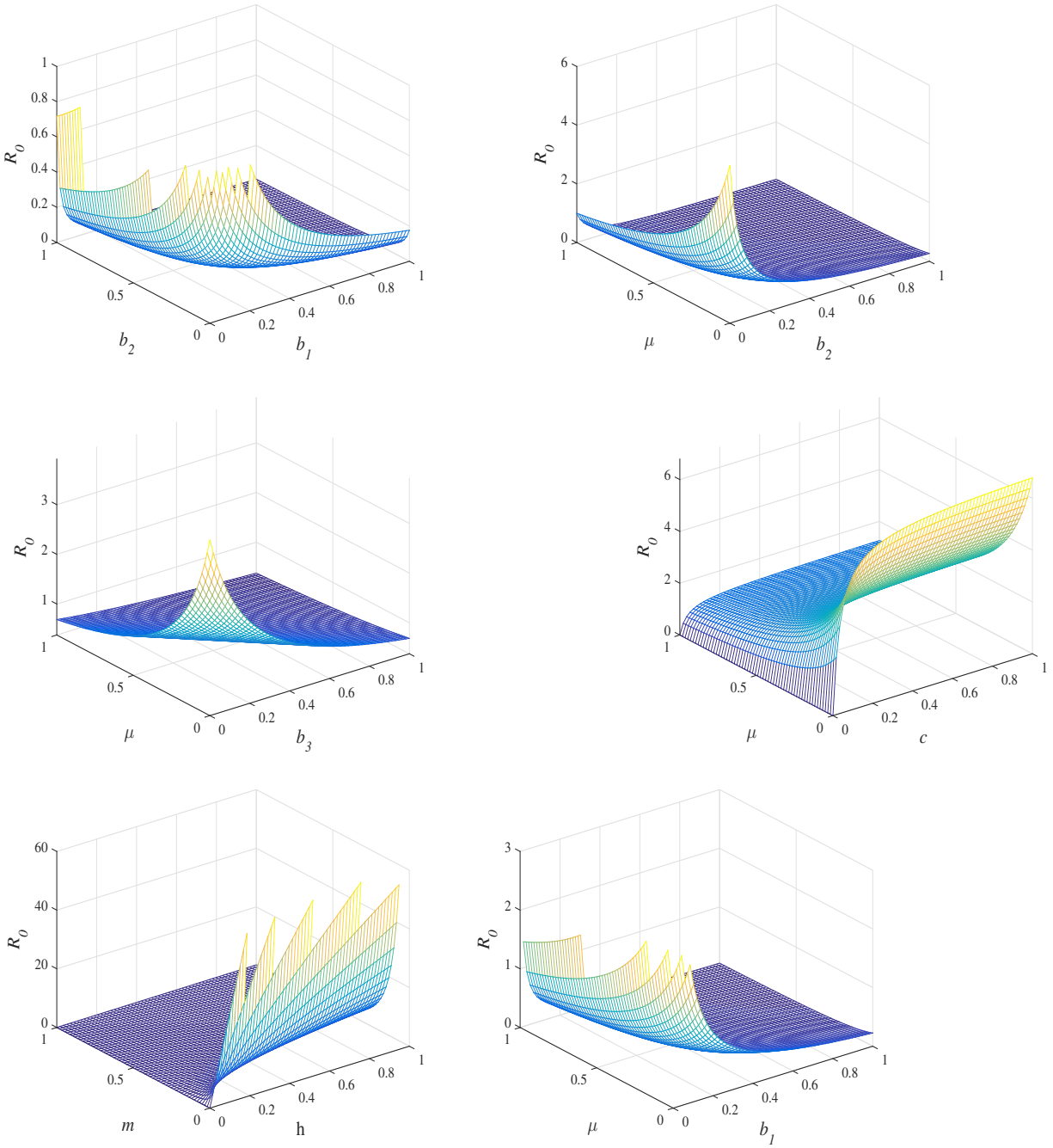

Figure 1: Behaviour of the basic reproduction number in three dimensions in relation to different model parameters.

5. Local Stability Analysis

In this section, we examine the model's (1) endemic equilibrium point (E^*) and without illness equilibrium point's (E^0) local and global stability analyses.

5.1. Local Stability Analysis of General Disease Model

Theorem 2. *If $R_0 < 1$, then the system's disease-free equilibrium point E^0 is locally asymptotically stable.*

Proof. The Jacobin matrix at disease free equilibrium is;

$$J(E^0) = \begin{bmatrix} -(m+b_1) & 0 & -\frac{hg}{m+b_1} & 0 & 0 \\ 0 & -(m+c+b_2) & \frac{hg}{m+b_1} & 0 & 0 \\ 0 & c & -(m+b_3+q+\mu) & 0 & 0 \\ b_1 & b_2 & b_3 & -(m+p) & 0 \\ 0 & 0 & q & p & -m \end{bmatrix}.$$

The three eigenvalues are $\lambda_1 = -m$, $\lambda_2 = -(m+p)$ and $\lambda_3 = -(m+b_1)$. To find the next eigenvalues, we use the 2×2 matrix and after algebraic manipulation we reached to

$$\lambda^2 + \lambda(2m + c + b_2 + b_3 + q + \mu) + (m + c + b_2)(m + b_3 + q + \mu) - \frac{hgc}{m + b_1} = 0. \quad (4)$$

When $R_0 > 1$, then the above equation $(m+c+b_2)(m+b_3+q+\mu) - \frac{hgc}{m+b_1} < 0$, This implies that Eq. (4) has a positive and negative root. Therefore, the disease-free equilibrium E^0 is unstable.

5.2. Global Asymptotic Stability of the Disease Free Equilibrium

In order to demonstrate the globally asymptotically stable nature of the disease-free equilibrium E^0, we examine the Lyapunov function for $R_0 \leq 1$,.

$$H(E, I) = B_1 E + B_2 I$$

The derivation of $H(E, I)$ with regrd to t gives,

$$\begin{aligned} \frac{dH}{dt} &= B_1 \frac{dE}{dt} + B_2 \frac{dI}{dt}, \\ \frac{dI}{dt} &= B_1\Big(\frac{hSI}{1+\alpha I} - (m+c+b_2)E\Big) + B_2\big(cE - (m+b_3+q+\mu)I\big), \\ &= B_1 \frac{hSI}{1+\alpha I} - B_1(m+c+b_2)E + B_2 cE - B_2(m+b_3+q+\mu)I, \end{aligned} \quad (5)$$

calculating the above equation which gives $B_1 = c$, and $B_2 = (m + c + b_2)$. so,

$$\begin{aligned} \frac{dH}{dt} &= \left[\frac{chS}{1+\alpha I} - (m+c+b_2)(m+b_3+q+\mu)\right] \\ &\leq \left[\frac{chS}{1+\alpha I} - (m+c+b_2)(m+b_3+q+\mu)\right] \\ &\leq \frac{chS_0}{R_0}\left[\frac{R_0 S}{S_0} - 1\right] I \leq 0. \end{aligned} \tag{6}$$

Furthermore $\frac{dH(E,I)}{dt} = 0$ if and only if $I = 0$. In light of this, the greatest compact invariant set in $\{(S,E,I,Q,R)|H(E,I) = 0\}$. When $R_0 \leq 1$, is the singleton E^0. Lasalle's invariance principle implies that E^0 is locally asymptotically stable.

5.3. Local Asymptotic Stability of Endemic Equilibrium

Theorem 3. *If $1 < R_0$ then (1) at endemic equilibrium, is locally asymptotically stable. The situation of endemicity state is unstable whenever $1 > R_0$.*

Proof. Jacobian matrix J at E^* shows that

$$J(E^*) = \begin{bmatrix} -\frac{hI^*}{1+\alpha I^*} - (m+b_1) & 0 & \frac{hS^*}{(1+\alpha I^*)^2} & 0 & 0 \\ \frac{hI^*}{1+\alpha I^*} & -(m+c+b_2) & \frac{hS^*}{(1+\alpha I^*)^2} & 0 & 0 \\ 0 & c & -(m+b_3+q+\mu) & 0 & 0 \\ b_1 & b_2 & b_3 & -(m+p) & 0 \\ 0 & 0 & q & p & -m \end{bmatrix}.$$

Eigenvalues of $J(E^*)$ are negative numbers that are $\lambda_1 = -m$, $\lambda_2 = -(m+p)$ then we only need to consider the roots of $\lambda^3 + B_1\lambda^2 + B_2\lambda + B_3 = 0$, where

$$\begin{aligned} B_1 &= \frac{hI_*}{1+\alpha I^*} + 3m + 2b_1 + b_3 + c + q > 0, \\ B_2 &= \left(\frac{hI^*}{1+\alpha I^*} + m + b_1\right)(2m + b_2 + b_3 + c + q + \mu) + (m+c+b_1)(m+b_3+q+\mu) - \frac{chS^*}{(1+\alpha I^*)^2} \\ &> \left(\frac{hI^*}{1+\alpha I^*} + m + b_1\right)(2m + b_2 + b_3 + c + q + \mu) > 0, \\ B_3 &= \left(\frac{hI^*}{1+\alpha I^*} + m + b_1\right)\left((m+c+b_1)(m+b_3+q+\mu) - \frac{chS^*}{(1+\alpha I^*)^2}\right) + \frac{ch^2 S^* I^*}{(1+\alpha I^*)^3} > 0. \end{aligned}$$

Based on the following relation $\frac{chS^*}{1+\alpha I^*} = (m+c+b_1)(m+b_3+q+\mu)$.
By a direct calculation, we have that $B_1B_2 - B_3 > 0$. Following Routh-harwitz criteria one can easily confirm endemic equilibrium E^* is locally asymptotically stable. This completes the proof.

6. Global Stability Analysis

Theorem 4. *If $R_0 > 1$, the endemic equilibrium E^* is globally asymptotically stable.*

Proof. Taking the subsystems in this case,

$$\begin{aligned} \frac{dS}{dt} &= g - \frac{hSI}{1+\alpha I} - (m+b_1)\,S, \\ \frac{dE}{dt} &= \frac{hSI}{1+\alpha I} - (m+c+b_2)\,E, \\ \frac{dI}{dt} &= cE - (m+b_3+q+\mu)\,I. \end{aligned} \tag{7}$$

The Jacobian matrix of the system is given as J.

$$J = \begin{bmatrix} -\frac{hI}{1+\alpha I} - (m+b_1) & 0 & -\frac{hs}{(1+\alpha)^2} \\ \frac{hI}{1+\alpha I} & -(m+c+b_2) & \frac{hs}{(1+\alpha)^2} \\ 0 & c & -(m+b_3+q+\mu) \end{bmatrix},$$

where $J^{|2|}$ stands for the second additive matrix of J. This matrix form exists in

$$J^{|2|} = \begin{bmatrix} -\frac{hI}{1+\alpha I} - k & \frac{hS}{(1+\alpha I)^2} & \frac{hS}{(1+\alpha)^2} \\ c & -\frac{hI}{1+\alpha I} - l & 0 \\ 0 & \frac{hI}{1+\alpha I} & -m \end{bmatrix}.$$

Entries of the last matrix are defined in the following way,
$k = 2m + c + b_1 + b_2$,
$l = 2m + b_1 + b_3 + q + \mu$,
$m = 2m + c + b_2 + b_3 + q + \mu$, Let us consider the function

$$X(x) = X(S,E,I) = diag\left\{1, \frac{E}{I}, \frac{E}{I}\right\}$$

Then,

$$X^{-1} = diag\left\{1, \frac{I}{E}, \frac{I}{E}\right\}, \quad X_f = diag\left\{0, \frac{\dot{E}}{I} - \frac{E\dot{I}}{I^2}, \frac{\dot{E}}{I} - \frac{E\dot{I}}{I^2}\right\}.$$

Direct calculation demonstrates that which can be seen further as

$$X_f X^{-1} = diag\left\{0, \frac{\dot{E}}{E} - \frac{\dot{I}}{I}, \frac{\dot{E}}{E} - \frac{\dot{I}}{I}\right\}.$$

$$XJ^{|2|}X^{-1} = \begin{bmatrix} x_{11} & \frac{hSI}{E(1+\alpha I)^2} & \frac{hSI}{E(1+\alpha I)^2} \\ \frac{Ec}{I} & x_{22} & 0 \\ 0 & \frac{hI}{1+\alpha I} & x_{33} \end{bmatrix}$$

Where
$x_{11} = \frac{-hI}{1+\alpha I} - (2m + c + b_1 + b_2)$,
$x_{22} = \frac{-hI}{1+\alpha I} - (2m + b_1 + b_3 + q + \mu)$,
$x_{33} = -(2m + c + b_2 + b_3 + q + \mu)$.
Thus, we are able to write

$$Q = X_f X^{-1} + X J^{|2|} X^{-1}.$$

It is simple to check if the matrix B has the specified form after values have been inserted.

$$Q = \begin{bmatrix} Q_{11} & Q_{12} \\ Q_{21} & Q_{22} \end{bmatrix}.$$

Take note that the entries in matrix Q are computed as

$$\begin{aligned} Q_{11} &= x_{11}, \\ Q_{12} &= \frac{hSI}{E(1+\alpha I)^2}, \quad \frac{hSI}{E(1+\alpha I)^2}, \\ Q_{21} &= \begin{bmatrix} \frac{cE}{I} \\ 0 \end{bmatrix}, \\ Q_{22} &= \begin{bmatrix} x_{22} + \frac{I\dot{E} - E\dot{I}}{IE} & 0 \\ \frac{hI}{1+\alpha I} & x_{33} + \frac{I\dot{E} - E\dot{I}}{IE} \end{bmatrix}. \end{aligned}$$

Let (u, v, w) be a vector in $\mathbb{R}^3$. Its norm $\|\cdot\|$ is defined as

$$\|(u, v, w)\| = \max\{|u|, |v| + |w|\}.$$

Let $\mu(Q)$ be the Lozinskiĭ measure with respect to this norm. Then

$$\mu(Q) \leq \sup\{g_1, g_2\},$$

where

$$\begin{aligned} g_1 &= \mu_1(Q_{11}) + \|Q_{12}\|, \\ g_2 &= \|Q_{21}\| + \mu_1(Q_{22}). \end{aligned}$$

Here $\|Q_{12}\|$ and $\|Q_{21}\|$ are matrix norms with respect to the ℓ_1 vector norm, and μ_1 denotes the Lozinskiĭ measure with respect to this ℓ_1 norm. Then

$$\begin{aligned} \mu_1(Q_{11}) &= -\frac{hI}{1+\alpha I} - (2m + c + b_1 + b_2), \\ \|Q_{21}\| &= \frac{cE}{I}, \\ \|Q_{12}\| &= \max\left\{ \frac{hSI}{E(1+\alpha I)^2}, \frac{hSI}{E(1+\alpha I)^2} \right\} = \frac{hSI}{E(1+\alpha I)^2}, \end{aligned}$$

and

$$\mu_1(Q_{22}) = \max\left\{\frac{\dot{E}}{E} - \frac{\dot{I}}{I} - \frac{hI}{1+\alpha I} - N, \quad \frac{hI}{1+\alpha I}, \quad \frac{\dot{E}}{E} - \frac{\dot{I}}{I} - K\right\} = \frac{\dot{E}}{E} - \frac{\dot{I}}{I} - \min(N, K).$$

Therefore, we have

$$g_1 = -\frac{hI}{1+\alpha I} - M + \frac{hSI}{E(1+\alpha I)^2},$$
$$g_2 = \frac{cE}{I} + \frac{\dot{E}}{E} - \frac{\dot{I}}{I} - \min(N, K).$$

From the proposed model (1.1), we get

$$\frac{\dot{E}}{E} = \frac{hSI}{E(1+\alpha I)} - (m + c + b_2),$$
$$\frac{\dot{I}}{I} = \frac{cE}{I} - (m + b_3 + q + \mu).$$

Then we have

$$\begin{aligned} g_1 &= -\frac{hI}{1+\alpha I} - (2m + c + b_1 + b_2) + \frac{hSI}{E(1+\alpha I)^2} + \left[\frac{hSI}{E(1+\alpha I)^2} - \frac{hSI}{E(1+\alpha I)}\right] \\ &\leq -\frac{hI}{1+\alpha I} - (m + b_1) + \frac{\dot{E}}{E}, \\ g_2 &= \frac{cE}{I} + \frac{\dot{E}}{E} - \frac{\dot{I}}{I} - \min(N, K) \\ &\leq \frac{\dot{E}}{E} - m. \end{aligned}$$

Since

$$\frac{cE}{I} = \frac{\dot{I}}{I} - (m + b_3 + q).$$

Furthermore, we obtain:

$$\mu(Q) \leq \sup\{g_1, g_2\} \leq \sup\left\{-\frac{hI}{1+\alpha I} - (m + b_1) + \frac{\dot{E}}{E}, \frac{\dot{E}}{E} - m\right\} \leq \frac{\dot{E}}{E} - m,$$

then

$$\frac{1}{t}\int_0^t \mu(Q)\, ds \leq \frac{1}{t}\int_0^t \left(\frac{\dot{E}}{E} - m\right) ds = \frac{1}{t}\ln\frac{E(t)}{E(0)} - m,$$

which implies $q \leq \frac{m}{2} < 0$. We know that positive equilibrium (S^*, E^*, I^*) is globally asymptotically stable.

In this section, it is described how the general disease model may be used to optimise control concepts.

7. Formulation of Optimal Control Problem

In order to design our control approach in this part, we take into consideration the general illness pandemic model. Through the use of the three control variables $u_1(t)$, which denote the effort that reduces the contact between the susceptibles and infectious individuals; $u_2(t)$, denote the rate at which infectious individuals are treated and $u_3(t)$, shows the vaccination coverage. Thus, by including the above-mentioned control variables, the general disease control model is created, and it looks like this:

$$\begin{cases} \dfrac{dS}{dt} = g - (1-u_1)\dfrac{hSI}{1+\alpha I} - (m+b_1)\,S - u_3 S, \\ \dfrac{dE}{dt} = (1-u_1)\dfrac{hSI}{1+\alpha I} - (m+c+b_2)\,E, \\ \dfrac{dI}{dt} = cE - (m+b_3+\mu)\,I - (1+u_2)\,qI, \\ \dfrac{dQ}{dt} = b_1 S + b_2 E + b_3 I - (m+p)Q, \\ \dfrac{dR}{dt} = (1+u_2)qI + pQ - mR + u_3 S. \end{cases} \tag{8}$$

The system (8) is subject to the nonnegative initial conditions [23, 24]

$$S(0) \;>\; 0,\; E \;\geq 0, I \;\geq 0, Q \;\geq 0 \;\text{ and } R(0) \;\geq\; 0.$$

We define the goal functional function, which aims to decrease the spread of the general disease infection, can be described as;

$$J(u_1(t), u_2(t), u_3(t)) \;=\; \int_0^{T_f} A_1 E + A_2 I - A_3 R + \frac{1}{2}\left[A_4 u_1^2(t) + A_5 u_2^2(t) + A_6 u_3^2(t)\right] \tag{9}$$

The values A_1, A_2 and A_3 are weight constants. The objective functional serves the purpose of minimising the number of affected individuals. In this way, we determine an optimal control triplet:

$$J(u_1^*(t), u_2^*(t), u_3^*(t)) = min\{J(u_1(t), u_2(t), u_3(t)) \in U\}. \tag{10}$$

According to the problem being considered, the control set is provided by
$U = \{u_1, u_2, u_3) : [0, T_f] \to [0, 1], (u_1, u_2, u_3) is\ a\ Labesgue\ measurable\}$.
Next, we demonstrate that the optimum control problem exists.

7.1. Existence of the Optimal Control Problem

Here, we provide proof that shows the control problem exists. For the optimum control issue, we provide the following definition of Hamiltonian H:

$$H \;=\; \mathcal{L}(E(t), I(t), R(t), u_1(t), u_2(t), u_3(t)) + \lambda_1 \frac{dS}{dt} + \lambda_2 \frac{dE}{dt} + \lambda_3 \frac{dI}{dt} + \lambda_4 \frac{dQ}{dt} + \lambda_5 \frac{dR}{dt} \tag{11}$$

Theorem 5. *For control issue* (4.1), *there is*

$$u^*(t) = (u_1^*(t), u_2^*(t), u_3^*(t)) \in U,$$

in such away that

$$min_{(u_1(t),u_2(t),u_3(t)\in U)} J(u_1(t), u_2(t), u_3(t)) = J(u_1^*, u_2^*, u_3^*(t)).$$

Proof. For the purpose of validating the optimal control rate, we used a variety of methodologies. Thus, each and every control and state variable has a positive value. Due to this, the issue is being reduced, So, $u_1(t), u_2(t)$ and $u_3(t)$ elaborates the required convexity of the goal functional and is satisfied. The collection of control variables $u_1, u_2, u_3 \in U$ is by definition convex and closed. There is a defined optimum system, Furthermore, it supplies the confidence regarding the solidity required for the verification of the optimal control system. Moreover, an integral in the practical purpose $A_1E+A_2I-A_3R+\frac{1}{2}(A_4u_1^2+A_5u_2^2+A_6u_3^2)$ which confirms the evidence, is convex on the control set U.

8. Optimality System

Theorem 6. *Given optimal controls* $u_1^*(t), u_2^*(t), u_3^*(t)$ *and solutions* S^*, E^*, I^*, Q^*, R^* *of the corresponding state system (8) there is adjoint variables* $\lambda_n(t), n = 1, ..., 5,$

$$\begin{cases} \frac{d\lambda_1}{dt} = (\lambda_1 - \lambda_2)(1-u_1)\frac{hI}{1+\alpha I} + (\lambda_1 - \lambda_4)b_1 + (\lambda_1 - \lambda_5)u_3 + m\lambda_1, \\ \frac{d\lambda_2}{dt} = -A_1 + (\lambda_2 - \lambda_3)c + (\lambda_2 - \lambda_4)b_2 + m\lambda_2, \\ \frac{d\lambda_3}{dt} = -A_2 + (\lambda_1 - \lambda_2)(1-u_1)\frac{hS}{(1+\alpha I)^2} + (\lambda_3 - \lambda_4)b_3 + (\lambda_3 - \lambda_5)(1+u_2)q + (m+\mu)\lambda_3 \\ \frac{d\lambda_4}{dt} = (\lambda_4 - \lambda_5)p + m\lambda_4 \\ \frac{d\lambda_5}{dt} = -A_3 + m\lambda_5, \end{cases}$$

with transversality conditions $\lambda_n(T_f) = 0, n = 1, ..., 5.$

Proof. When we consider the values as $S(t) = S^*, E(t) = E^*, I(t) = I^*, Q(t) = Q^*$, and $R(t) = R^*$ and differentiate the Hamiltonian with respect to state variables $S(t), E(t), I(t), Q(t)$ *and* $R(t)$, respectively, we get the adjoint system (12) with transversality conditions $\lambda_n(t) = 0, n = 1, 2, ..., 5$. In coming part, we develop the principles of optimal control variables as follows: while using optimal conditions for solution $\frac{\partial H}{\partial u_1} = 0, \frac{\partial H}{\partial u_2} = 0$ and $\frac{\partial H}{\partial u_3} = 0$ on the inside of the control setup.

Lastly, we employ the control area characteristic while writing.

$$u_1(t) = \frac{(\lambda_2 - \lambda_1)}{A_4}\frac{hSI}{1+\alpha I},$$

$$\begin{aligned} u_2(t) &= \frac{(\lambda_3-\lambda_5)qI}{A_5}, \\ u_3(t) &= \frac{(\lambda_1-\lambda_5)S}{A_6}. \end{aligned} \tag{12}$$

As one can see, the equation (12) for $U^* = (u_1^*, u_2^*, u_3^*)$ is made reference to as a representation of optimal controls. State variables and optimum control are obtained by solving the optimality system. When values are entered for u_1, u_2 and u_3 in the system, we obtain the underlying syste,:

$$\begin{cases} \frac{dS^*}{dt} = g - \frac{hS^*I^*}{1+\alpha I^*} - (m+b_1)\,S^* - (\frac{(\lambda_1-\lambda_5)S}{A_6})S^*, \\ \frac{dE^*}{dt} = (1-(\frac{(\lambda_2-\lambda_1)}{A_4}\frac{hSI}{1+\alpha I}))\frac{hS^*I^*}{1+\alpha I^*} - (m+c+b_2)\,E^*, \\ \frac{dI^*}{dt} = cE^* - \left(m+b_3+(1+(\frac{(\lambda_3-\lambda_5)qI}{A_5}))q+\mu\right)I^*, \\ \frac{dQ^*}{dt} = b_1S^* + b_2E^* + b_3I^* - (m+p)Q^*, \\ \frac{dR^*}{dt} = (1+(\frac{(\lambda_3-\lambda_5)qI}{A_5}))qI^* + pQ^* - mR^* + (\frac{(\lambda_1-\lambda_5)S}{A_6})S^*. \end{cases} \tag{13}$$

The next section includes several numerical simulations. To verify the analytical findings from the previous section. The numerical simulations are also briefly discussed.

9. Numerical Results

9.1. Numerical Simulations for the Problem (Without Control Variables)

The numerical simulations used to validate the results of analysis examined in the earlier chapters are the focus of this portion of the thesis. We employ the widely established Runge-Kutta method of fourth order ($RK4$). In the beginning, we run numerical simulations for a case in which an area is free of disease, i.e the so-called condition devoid of infections. The threshold quantity's value is assumed to be smaller than unity by selecting parameter values in the model under consideration.

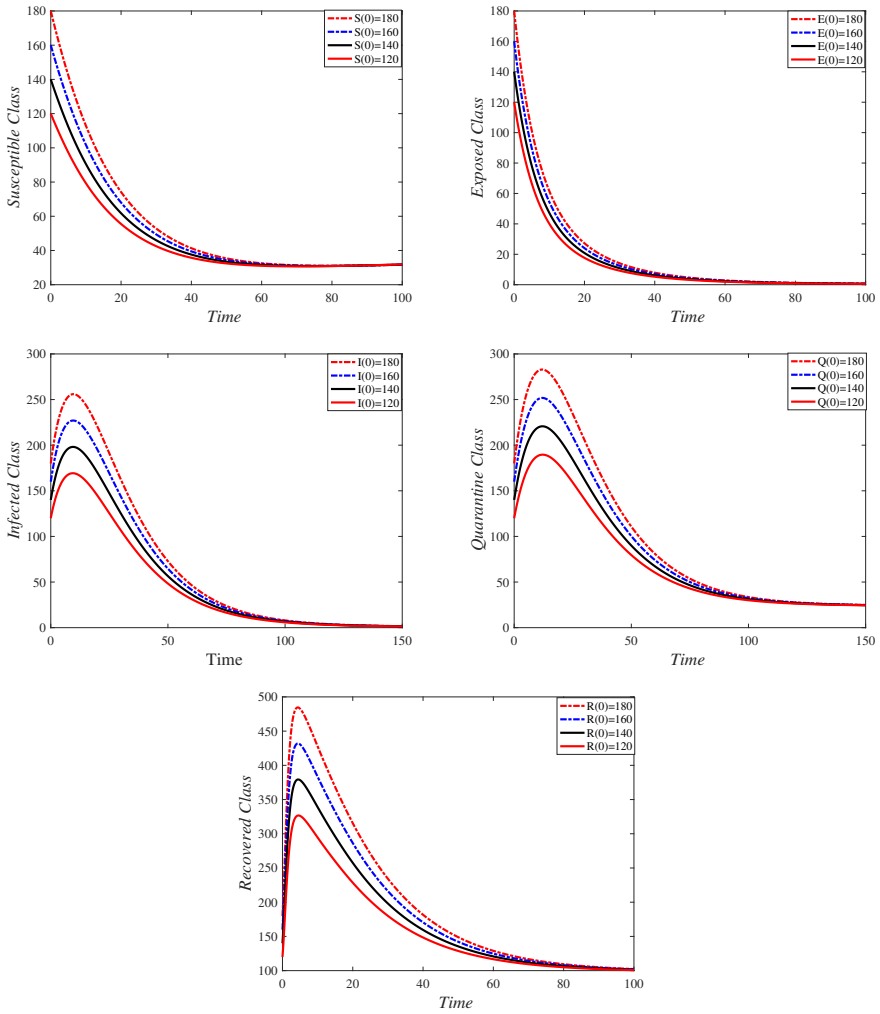

Figure 2: Dynamical behaviour of the trajectories of the total classes of the model for the no-infection state.

In Fig. (2) (Susceptible population graph) we plot the trajectories of the susceptible compartment of the model under consideration for the infection-free condition versus time t, for varied initial sizes of the compartment. From this figure, we observe that the susceptible population decreases and gradually tend to the no-disease state S^0. We also observe that this equilibrium is nonzero. It means that there will always be chance to people to catch the disease, which is biologically relevant. (Exposed population graph) demonstrates how the exposed class of infection behave dynamically. The class is rapidly decreasing at the no illness state. As time increases, the class becomes closer to the zero state, or the equilibrium free of sickness. In Fig. (Infected population graph) we depict the infected class. At the disease-free condition, there is a quickly increase for first few weeks in the class. As time increases, the class becomes closer to the zero condition,

or the equilibrium free from sickness. In other words, the infection population reaches its convergence at the zero condition as time goes on. This agrees with the value of I^0 already determined for the no-infection state. In Fig. (Quarantine population graph) the quarantine class's solution curve is displayed. The class is growing over time and eventually converges to an infection-free state, demonstrating that this class's equilibrium is non-zero. In Fig. (Recovered population graph) different beginning conditions are used to run the simulations. As time goes on, we see a sharp rise in the recovered population and a tendency of the class towards zero, the no-infection equilibrium condition. Now, we consider the case of persistence of the disease in a community. For this we take the values: $g = 10,\ h = 0.01,\ m = 0.0124,\ b_1 = 0.05,\ c = 0.04,\ b_2 = 0.0246,\ b_3 = 0.015,\ q = 0.2,\ \mu = 0.2,\ p = 0.4,\ \alpha = 0.2$ and perform numerical simulations.

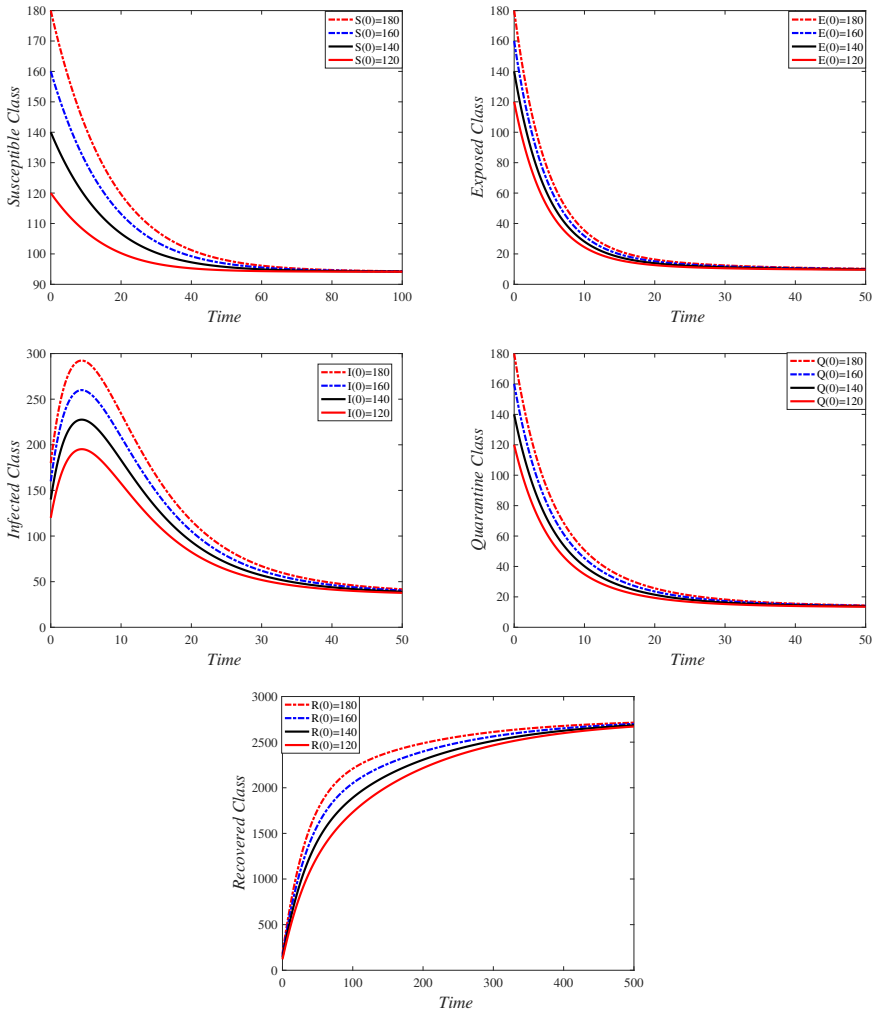

Figure 3: Dynamical behaviour of the trajectories of the total classes of the model for the infection state.

Fig. (3) displays the infected compartment in the event that the disease continues to spread throughout a community for different beginning compartment sizes. The compartment is initially shown to be rising; as time goes on, the compartment falls and converges to the illness endamic state. This validates our analytical findings. While in the last figure (recovered population graph) show the picture of the recovered population versus time for various initial conditions. We see that throughout the first several weeks, this class grows and then progressively approaches the endemic stability threshold.

9.2. Numerical Simulations for the Optimal Control Problem

We numerically solve the optimal control model (8) using the Runge-Kutta method of order 4. The parametric values are taken as: $A_1 = 2,\ , A_2 = 3,\ A_3 = 4,\ A_4 = 5,\ A_5 = A_6 = 1,\ g = 10,\ h = 0.00245,\ m = 0.0124,\ b_1 = 0.4,\ c = 0.4,\ b_2 = 0.5,\ b_3 = 0.45,\ q = 0.5,\ \mu = 0.023,\ p = 0.4,\ \alpha = 0.2,$ The Fig. (4) are the solution curves of the susceptible class both in the absence and presence of the optimal control parameters. We observe from the figure, that the susceptible population can be increased once one applies the control stratifies. In other words, the number of susceptible individuals increase when the control measures are adopted. The figure also show that the class $S(t)$ decreases whenever these measures are avoided.

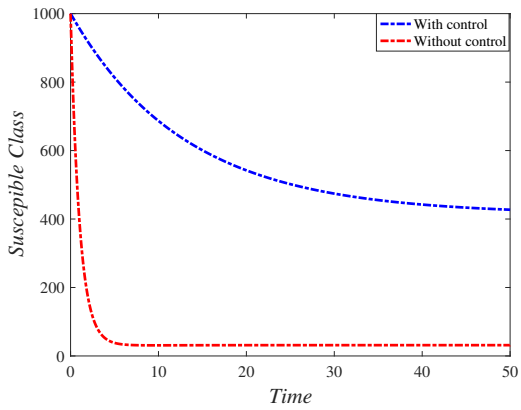

Figure 4: Solution curves of the trajectories of susceptible class of the model under consideration with and without control parameters.

Plotted in the second panel of Fig. (5) are the trajectories of the exposed and quarantine classes both in the absence and presence of the control measures. It is observed from both figures that the population can be decreased with the application of the control measures, which is the aim of the optimal control problem.

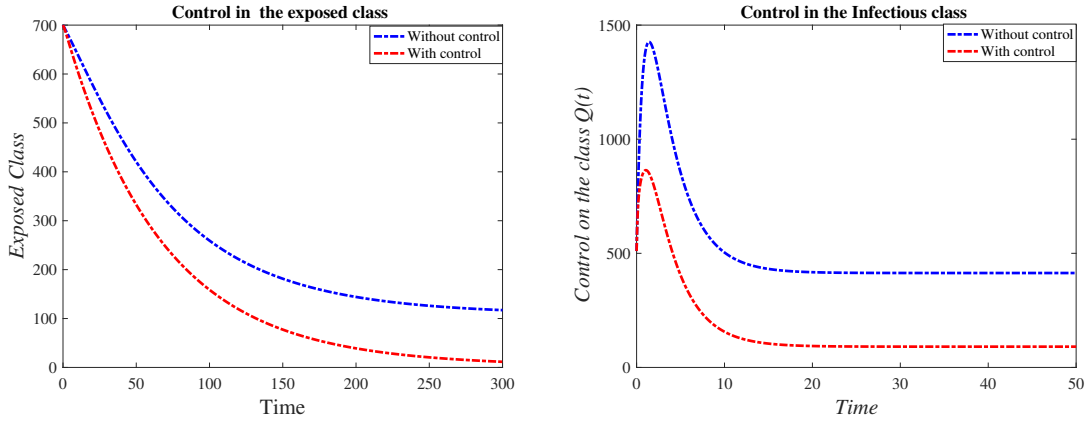

Figure 5: Solution curves of the trajectories of various classes of the model under consideration with and without control parameters.

In the same way, other panels of the figure Fig. (6) shows that the infected population can be decreased once the control measures are adopted. Similarly the recovered populations are enhanced with the control measures suggested in our control problem.

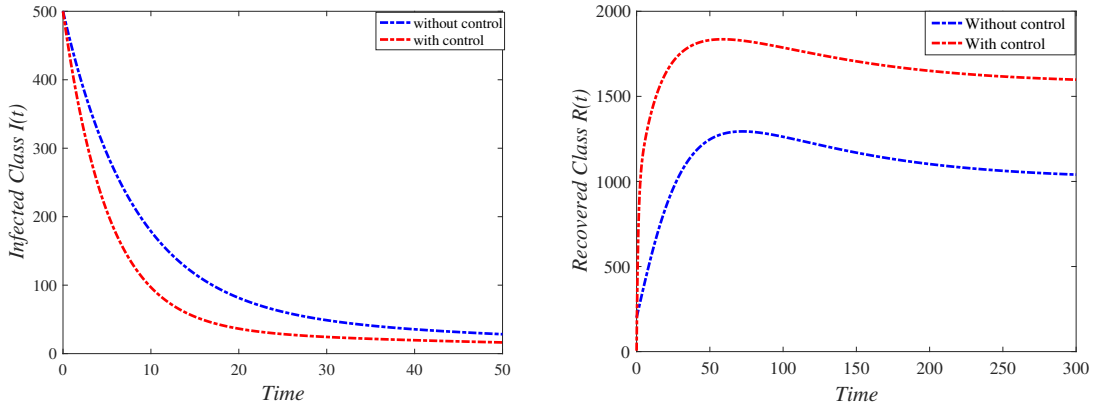

Figure 6: Solution curves of the trajectories of various classes of the model under consideration with and without control parameters.

10. Phase Portrait Study for Proposed Model

The phase portrait analysis provides a comprehensive visualization of the system's trajectories under both controlled and uncontrolled scenarios, highlighting the impact of intervention strategies on disease dynamics. System of figure (7) illustrates the interplay between different populations, demonstrating distinct behavioral patterns. In the absence of control measures, trajectories diverge toward higher infection levels, aligning with the endemic equilibrium. Conversely, with optimal controls u_1, u_2, and u_3 applied, trajectories

converge toward regions of reduced infection density, reflecting the efficacy of interventions in steering the system closer to the disease-free equilibrium. Similarly, System of (8) also compares the temporal evolution of different compartments, revealing that control implementation suppresses E while elevating Q, consistent with enhanced quarantine efforts. The shrinking of phase space near endemic states under control shows stable dynamics, conforming the global stability that has been mathematically proven. The visualizations above show how control parameters influence the attractors of the system, proving their role in reducing the severity of outbreaks. The convergence patterns we witness confirm the theoretical stability criteria of R_0, showing that efficient strategies can readily break transmission networks, as testified by fewer cycles and faster stabilization. This geometric analysis is corroborated by numerical results, providing easy-to-interpret evidence of the model's ability to make predictions under intervention.

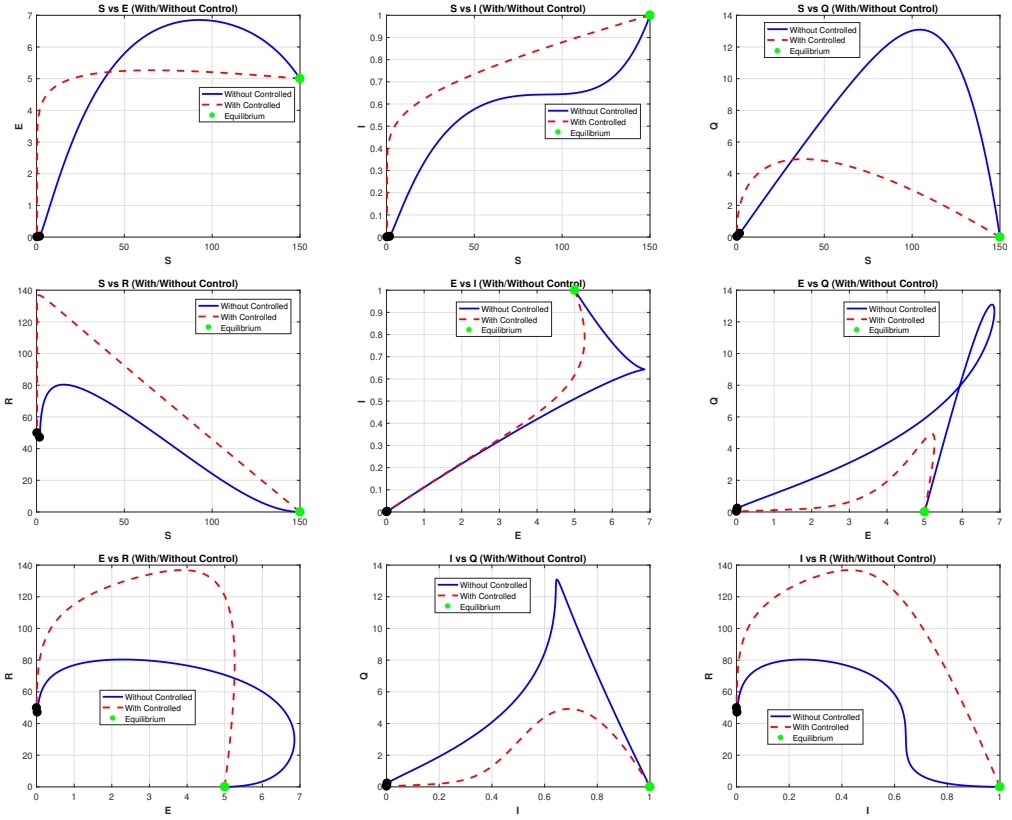

Figure 7: Phase Photrate system

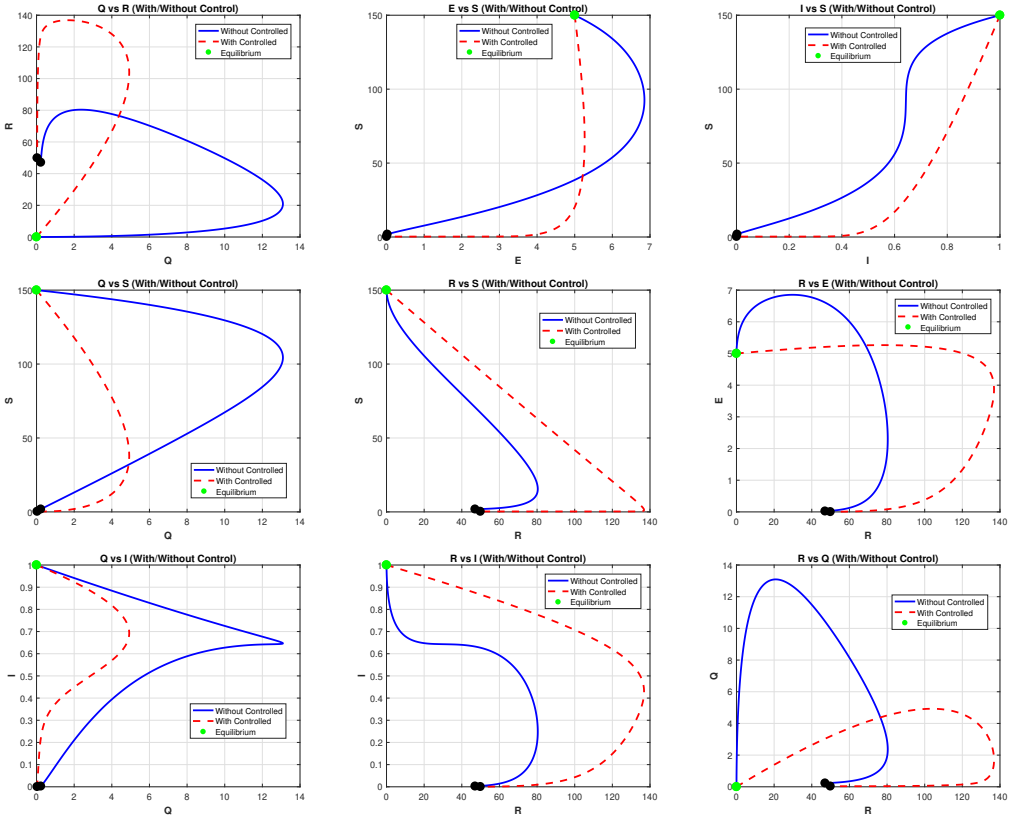

Figure 8: Phase Photrate system

11. Conclusions

We examined the mathematical model of epidemics in this manuscript. We talked about a few key characteristics, such as the investigated model's solutions' positivity and boundedness within a biologically acceptable range. We calculated the fundamental threshold number R_0 in order to talk about the stability analysis of the potential non-trivial equilibria of the suggested model. This was accomplished by utilising a well-known the next-generation techniques for technology. We've set criteria for both the local and global stability of the simulation under consideration's no-infection and disease-endemic states. Using the linearization technique, we conducted the studies of local stability. The Castillo-Chavez approach and geometric method are used accordingly to explore the global stability assessments of a disease-endemic condition and the no-infection state. Research has shown that when the fundamental threshold number R_0 takes values smaller or larger than unity, the no-infection (endemic) condition is maintained on a global and local scale. In order to stop a general illness infection from spreading, we include three control variables: $u_1(t)$, which denote the effort that reduces the contact between the susceptible and infectious individuals; $u_2(t)$, denote the rate at which infectious individuals are treated

and $u_3(t)$, shows the vaccination coverage. We numerically solve the proposed model using the widely recognised fourth order Runge-Kutta (RK-4) approach. Our numerically obtained results well support the analytical findings. The phase portrait analysis further demonstrates how system trajectories evolve under different control strategies, visually confirming the stabilization toward disease-free equilibrium when interventions are applied. The current work may be extended to fractional order differential equations and various approaches can be used to study the transmission dynamics of a general infection. Work on such problems is under investigation and will be reported in a near publication.

Acknowledgements

Manuel De la Sen is thankful to the Basque Government, Grants IT1555-22, for the financial support.

References

[1] A. Omame, H. Rwezaura, M. L. Diagne, S. C. Inyama, and J. M. Tchuenche. Covid-19 and dengue co-infection in brazil: optimal control and cost-effectiveness analysis. *European Physical Journal Plus*, 136(10):1090, 2021.

[2] A. Abidemi, Z. M. Zainuddin, and N. A. B. Aziz. Impact of control interventions on covid-19 population dynamics in malaysia: a mathematical study. *European Physical Journal Plus*, 136:1–35, 2021.

[3] K. Wang, A. Fan, and A. Torres. Global properties of an improved hepatitis b virus model. *Nonlinear Analysis: Real World Applications*, 11(4):3131–3138, 2010.

[4] X. Liu, M. U. Rahman, S. Ahmad, D. Baleanu, and Y. N. Anjum. A new fractional infectious disease model under the non-singular mittag–leffler derivative. *Waves in Random and Complex Media*, pages 1–27, 2022.

[5] M. G. M. Gomes, A. Margheri, G. F. Medley, and C. Rebelo. Dynamical behaviour of epidemiological models with sub-optimal immunity and nonlinear incidence. *Journal of Mathematical Biology*, 51:414–430, 2005.

[6] O. Zakary, M. Rachik, and I. Elmouki. On the analysis of a multiregions discrete sir epidemic model: an optimal control approach. *International Journal of Dynamics and Control*, 5:917–930, 2017.

[7] S. Ullah, M. F. Khan, S. A. A. Shah, M. Farooq, M. A. Khan, and M. B. Mamat. Optimal control analysis of vector-host model with saturated treatment. *European Physical Journal Plus*, 135(10):1–25, 2020.

[8] G. Zaman, Y. H. Kang, and I. H. Jung. Stability and optimal vaccination of an sir epidemic model. *BioSystems*, 93:240–249, 2008.

[9] A. V. Kamyad, R. Akbari, and A. Heydari. Mathematical modeling of transmission dynamics and optimal control of vaccination and treatment for hepatitis b virus. *Computational and Mathematical Methods in Medicine*, pages 1–15, 2004.

[10] G. Zaman, Y. H. Kang, and I. H. Jung. Optimal treatment of an sir epidemic model with time delay. *BioSystems*, 98:43–50, 2009.

[11] I. Shah, H. Alrabaiah, and B. Ozdemir. Using advanced analysis together with fractional order derivative to investigate a smoking tobacco cancer model. *Results in Physics*, 51:106700, 2023.

[12] S. Ahmad, N. Ahmad, and I. Shah. Stability and sensitivity analysis of cyberattack propagation models in computer networks. *European Journal of Pure and Applied Mathematics*, 18(3):6336, 2025.

[13] I. Shah, I. Ali, A. Ali, I. Ahmad, S. Islam, G. Rasool, S. Formanova, and M. Kallel. Optimal control and sensitivity analysis of a mathematical model for mdr-tb transmission with advanced treatment strategies. *European Physical Journal Plus*, 140(6):1–15, 2025.

[14] I. Ullah, S. Ahmad, M. Arfan, and M. De la Sen. Investigation of fractional order dynamics of tuberculosis under caputo operator. *Fractal and Fractional*, 7(4):300, 2023.

[15] H. Inaba. Mathematical analysis of an age-structured sir epidemic model with vertical transmission. *Discrete and Continuous Dynamical Systems - Series B*, 6:69, 2006.

[16] X. Liu and L. Yang. Stability analysis of an seiqv epidemic model with saturated incidence rate. *Nonlinear Analysis: Real World Applications*, 13(6):2671–2679, 2012.

[17] L. Esteva and M. Matias. A model for vector transmitted diseases with saturation incidence. *Journal of Biological Systems*, 9(4):235–245, 2001.

[18] S. R. Chawla, S. Ahmad, and A. Khan. Sensitivity and bifurcation analysis of pine wilt disease with harmonic mean type incidence rate. *Physica Scripta*, 97(5):055006, 2022.

[19] A. Korobeinikov and P. K. Maini. Non-linear incidence and stability of infectious disease models. *Mathematical Medicine and Biology*, 22(2):113–128, 2005.

[20] M. D. Samsuzzoha, M. Singh, and D. Lucy. Uncertainty and sensitivity analysis of the basic reproduction number of a vaccinated epidemic model of influenza. *Applied Mathematical Modelling*, 37(3):903–915, 2013.

[21] H. S. Rodrigues, M. T. T. Monteiro, and D. F. M. Torres. Seasonality effects on dengue: basic reproduction number, sensitivity analysis and optimal control. *Mathematical Methods in the Applied Sciences*, 39(16):4671–4679, 2016.

[22] V. Capasso and G. Serio. A generalization of the kermack-mckendrick deterministic epidemic model. *Mathematical Biosciences*, 42(1-2):43–61, 1978.

[23] S. R. Chawla, S. Ahmad, W. Albalawi, A. Khan, I. Shah, and M. R. Eid. Stability analysis of a modified general seir model with harmonic mean type of incidence rate. *Alexandria Engineering Journal*, 127:1183–1192, 2025.

[24] A. Korobeinikov and P. K. Maini. Non-linear incidence and stability of infectious disease models. *Mathematical Medicine and Biology*, 22(2):113–128, 2005.